INTERNATIONAL JOURNAL FOR NUMERICAL METHODS IN ENGINEERING
Int. J. Numer. Meth. Engng 2001; **52**:1029–1043 (DOI: 10.1002/nme.255)

Convergence study of the truncated Karhunen–Loeve expansion for simulation of stochastic processes

S. P. Huang, S. T. Quek and K. K. Phoon*,†

Department of Civil Engineering, National University of Singapore, Block E1A #07-03, 1 Engineering Drive 2, Singapore 117576

SUMMARY

A random process can be represented as a series expansion involving a complete set of deterministic functions with corresponding random coefficients. Karhunen–Loeve (K–L) series expansion is based on the eigen-decomposition of the covariance function. Its applicability as a simulation tool for both stationary and non-stationary Gaussian random processes is examined numerically in this paper. The study is based on five common covariance models. The convergence and accuracy of the K–L expansion are investigated by comparing the second-order statistics of the simulated random process with that of the target process. It is shown that the factors affecting convergence are: (a) ratio of the length of the process over correlation parameter, (b) form of the covariance function, and (c) method of solving for the eigen-solutions of the covariance function (namely, analytical or numerical). Comparison with the established and commonly used spectral representation method is made. K–L expansion has an edge over the spectral method for highly correlated processes. For long stationary processes, the spectral method is generally more efficient as the K–L expansion method requires substantial computational effort to solve the integral equation. The main advantage of the K–L expansion method is that it can be easily generalized to simulate non-stationary processes with little additional effort. Copyright © 2001 John Wiley & Sons, Ltd.

KEY WORDS: Karhunen–Loeve expansion; stationary Gaussian process; non-stationary Gaussian process; stochastic series representation; simulation; covariance models

1. INTRODUCTION

Engineering parameters such as environmental loads and mechanical properties of the resisting media are sometimes treated as random processes or fields for reliability analysis. The randomness must be realistically represented to achieve a meaningful solution to the specific reliability problem. A random process can be represented as a series expansion involving a complete set of deterministic functions with corresponding random coefficients. This method provides a second-moment characterisation in terms of random variables and deterministic functions. There are several such series that are widely in use. A commonly used series

*Correspondence to: Kok-Kwang Phoon, Department of Civil Engineering, National University of Singapore, Block E1A #07-03, 1 Engineering Drive 2, Singapore 117576
†E-mail: cvepkk@nus.edu.sg

involves spectral expansion [1, 2], in which the random coefficients are uncorrelated only if the random process is assumed stationary and the length of the random process is infinite or periodic [3]. The deterministic functions in the spectral expansion method consist of sine and cosine functions. Zhang and Ellingwood [4] proposed another orthogonal series expansion using Legendre polynomials as the deterministic basis function. However, the random coefficients in the expansion are correlated random variables. Other polynomials have also been used [5]. The use of Karhunen–Loeve (K–L) expansion with orthogonal deterministic basis functions and uncorrelated random coefficients has generated interest because of its bi-orthogonal property, that is, both the deterministic basis functions and the corresponding random coefficients are orthogonal. This allows for the optimal encapsulation of the information contained in the random process into a set of discrete uncorrelated random variables [6].

In the K–L expansion method, the orthogonal deterministic basis function and its magnitude are, respectively, the eigenfunction and eigenvalue of the covariance function. Note that the covariance function need not belong to stationary processes. Simulation using K–L expansion can be made efficient if an analytical pre-processing step of the eigen-solution is available, whereby the computational effort is drastically reduced while safeguarding accuracy [6]. The eigen-solution of the covariance function involves the solution of an integral equation. However, only a limited number of analytical eigen-solutions are available. For most covariance functions, the eigen-solution has to be evaluated numerically. Although some studies have been performed on the K–L expansion method [6, 7], important issues concerning its practical use as a simulation tool remain unanswered. The objective of this paper is to examine the practicality of implementing the K–L method as a general tool for simulating both stationary and non-stationary Gaussian processes. The effect of using analytical and numerical eigen-solutions on the second-order statistics of the simulated processes is compared. Factors that affect convergence and accuracy, such as the ratio of the length of the process over the correlation parameter, the form of the covariance function, and the number of terms used in the K–L expansion, are also examined. The K–L expansion is also compared with the spectral representation method for both weakly and highly correlated processes, both analytically and numerically. Finally, an example of a non-stationary Gaussian process is provided to illustrate the potential of K–L expansion in the direct simulation of more complicated processes.

2. KARHUNEN–LOEVE EXPANSION

2.1. Introduction

Consider a random process $\varpi(x,\theta)$ defined on a probability space (Ω, A, P) and indexed on a bounded domain D. Assume that the process has a mean $\bar{\varpi}(x)$ and a finite variance, $E[\varpi(x,\theta)-\bar{\varpi}(x)]^2$, that is bounded for all $x \in D$. The process can be expressed as [8]

$$\varpi(x,\theta) = \bar{\varpi}(x) + \sum_{i=1}^{\infty} \sqrt{\lambda_i}\xi_i(\theta) f_i(x) \tag{1}$$

in which λ_i and $f_i(x)$ are the eigenvalues and eigenfunctions of the covariance function $C(x_1,x_2)$. By definition, $C(x_1,x_2)$ is bounded, symmetric and positive definite. Following

Mercer's Theorem [8], it has the following spectral or eigen-decomposition:

$$C(x_1,x_2)=\sum_{i=1}^{\infty}\lambda_i f_i(x_1)f_i(x_2) \tag{2}$$

and its eigenvalues and eigenfunctions are the solution of the homogeneous Fredholm integral equation of the second kind given by

$$\int_D C(x_1,x_2)f_i(x_1)\,\mathrm{d}x_1=\lambda_i f_i(x_2) \tag{3}$$

Equation (3) arises from the fact that the eigenfunctions form a complete orthogonal set satisfying the equation

$$\int_D f_i(x)f_j(x)\,\mathrm{d}x=\delta_{ij} \tag{4}$$

where δ_{ij} is the Kronecker-delta function.

The parameter $\xi_i(\theta)$ in Equation (1) is a set of uncorrelated random variables which can be expressed as

$$\xi_i(\theta)=\frac{1}{\sqrt{\lambda_i}}\int_D[\varpi(x,\theta)-\bar{\varpi}(x)]f_i(x)\,\mathrm{d}x \tag{5}$$

with mean and covariance function given by

$$\begin{aligned} E[\xi_i(\theta)] &= 0 \\ E[\xi_i(\theta)\xi_j(\theta)] &= \delta_{ij} \end{aligned} \tag{6}$$

The series expansion in Equation (1), referred to as the K–L expansion, provides a second-moment characterization in terms of uncorrelated random variables and deterministic orthogonal functions. It is known to converge in the mean square sense for any distribution of $\varpi(x,\theta)$ [8]. For practical implementation, the series is approximated by a finite number of terms, say M, giving

$$\hat{\varpi}(x,\theta)=\bar{\varpi}(x)+\sum_{i=1}^{M}\sqrt{\lambda_i}\xi_i(\theta)f_i(x) \tag{7}$$

The corresponding covariance function is given by

$$\hat{C}(x_1,x_2)=\sum_{i=1}^{M}\lambda_i f_i(x_1)f_i(x_2) \tag{8}$$

Ghanem and Spanos [6] have shown this truncated series to be optimal; that is, the mean square approximation error is minimized.

If $\varpi(x,\theta)$ is further restricted to a zero-mean Gaussian process, then the appropriate choice of $\{\xi_1(\theta),\xi_2(\theta)\cdots\}$ is a vector of zero-mean uncorrelated Gaussian random variables. The variables can be generated by available established subroutines and then multiplied by the

eigenfunctions and eigenvalues derived from eigen-decomposition [Equation (3)] of the target covariance model. The value of M is hence governed by the accuracy of the eigen-pairs in representing the covariance function rather than the number of random variables.

In view of the fact that Equation (7) is a summation of Gaussian random variables, the process would be Gaussian distributed. Taking the expectation of Equation (7), the mean of the simulated process is $\bar{\varpi}(x)$. The second-order statistics of the target process are also reproduced by the simulated process since the ensemble covariance function of the simulated random process $\hat{\varpi}(x,\theta)$ can be written as

$$\begin{aligned}\hat{C}_e(x_1,x_2) &= E\left[\{\hat{\varpi}(x_1,\theta)-\bar{\varpi}(x)\}\{\hat{\varpi}(x_2,\theta)-\bar{\varpi}(x)\}\right]\\ &= E\left[\sum_{i=1}^{M}\sqrt{\lambda_i}\xi_i(\theta)f_i(x_1)\sum_{j=1}^{M}\sqrt{\lambda_j}\xi_j(\theta)f_j(x_2)\right]\\ &= \sum_{i=1}^{M}\sum_{j=1}^{M}\sqrt{\lambda_i}\sqrt{\lambda_j}f_i(x_1)f_j(x_2)E[\xi_i(\theta)\xi_j(\theta)] \qquad (9)\end{aligned}$$

By virtue of Equation (6),

$$\hat{C}_e(x_1,x_2)=\sum_{i=1}^{M}\lambda_i f_i(x_1)f_i(x_2)=\hat{C}(x_1,x_2) \qquad (10)$$

As $M\to\infty$, Equation (10) converges to Equation (2).

The key to K–L expansion is therefore to obtain the eigenvalues and eigenfunctions of the covariance function by solving the homogeneous Fredholm integral equation of the second kind in Equation (3). The integral equation can be solved analytically only in special circumstances. In most cases, the analytical solution of the integral equation is not tractable and the numerical method is the only recourse. To apply K–L as a general simulation tool, it is therefore very important to study the practicality and accuracy of solving the Fredholm integral equation numerically.

2.2. Analytical solution of Fredholm integral equation

For some classes of covariance function, Equation (3) can be differentiated twice with respect to x_2 analytically. The resulting differential equation is then solved analytically. To satisfy the boundary conditions, the solution is substituted into Equation (3) to yield the eigenvalues [8]. The commonly used random processes that fall into this category are as follows:

(1) *Stationary process with rational spectra*. An example in this class is the first-order Markov process that has the covariance function

$$C(x_1,x_2)=\sigma^2 e^{-|x_1-x_2|/b} \qquad (11)$$

where σ^2 is the variance and b is the correlation parameter.

(2) *Band-limited stationary process*. The spectrum of such a random process is not rational but the procedure described above can be used.

(3) *Special class of non-stationary processes*. The Wiener–Levy and the Brown–Bridge random processes are two known cases where Equation (3) can be solved by converting to a boundary-value problem.

2.3. Numerical solution of Fredholm integral equation

For random processes where the analytical solution of the integral equation for K–L expansion is not tractable, a numerical solution is necessary. There are two commonly used classes of numerical methods:

(1) *Integration formulae-based methods.* Examples of such simple and direct methods include the quadrature method and product-integration method [7].

(2) *Expansion methods*. Expansion methods are best suited for kernels that are analytically defined. Each eigenfunction is approximated by a linear combination of chosen basis functions. This will result in an error in Equation (3), which can be minimized using methods such as Galerkin, collocation or Rayleigh–Ritz. In this paper, the Galerkin method is used as the error is minimized over the entire domain rather than at pre-selected collocated points. For the case where the kernel $C(x_1,x_2)$ is symmetric, bounded and positive definite, the Galerkin method and the Rayleigh–Ritz method are, in fact, identical. The steps involved in employing Galerkin method are as follows:

(a) select a set of N basis functions, say $\phi_1(x), \phi_2(x), \ldots, \phi_N(x)$
(b) each eigenfunction is approximated by a linear combination of these functions

$$f_i(x) = \sum_{k=1}^{N} d_{ik}\phi_k(x) \tag{12}$$

where d_{ik} are constant coefficients for the ith eigenfunction.

(c) Substitute Equations (11) and (12) into Equation (3) and set the error in Equation (3) to be orthogonal to each basis function (denoted by subscript j) to obtain the following equation:

$$\sum_{k=1}^{N} d_{ik}\left[\int_D\int_D C(x_1,x_2)\phi_k(x_1)\phi_j(x_2)\,\mathrm{d}x_1\,\mathrm{d}x_2\right] - \lambda_i\sum_{k=1}^{N} d_{ik}\left[\int_D \phi_k(x_2)\phi_j(x_2)\,\mathrm{d}x_2\right] = 0 \tag{13}$$

or

$$\mathbf{AD} = \Lambda\mathbf{BD} \tag{14}$$

in which the components in all the $N\times N$ matrices are:

$$A_{kj} = \int_D\int_D C(x_1,x_2)\phi_k(x_1)\phi_j(x_2)\,\mathrm{d}x_1\,\mathrm{d}x_2 \tag{15}$$

$$D_{ik} = d_{ik} \tag{16}$$

$$\Lambda_{ij} = \delta_{ij}\lambda_j \tag{17}$$

$$B_{kj} = \int_D \phi_k(x_2)\phi_j(x_2)\,\mathrm{d}x_2 \tag{18}$$

The generalized algebraic eigenvalue problem of Equation (14) may be solved to obtain the eigenvalues λ_i and coefficients d_{ik}. In this paper, 5–10th degree polynomials are chosen as basis functions, depending on the number of terms in the K–L expansion (M). The Galerkin scheme described above is known to produce lower bound solutions for the eigenvalues and is more accurate for eigenvalues than for eigenfunctions [6].

2.4. Relation between K–L expansion and spectral representation method

Consider the case where the process to be represented is stationary and the observation interval is infinite. Equation (3) becomes

$$\lambda f(x_2) = \int_{-\infty}^{\infty} C(x_2 - x_1) f(x_1)\, \mathrm{d}x_1, \quad -\infty < x_2 < \infty \tag{19}$$

Equation (19) is analogous to the convolution integral with input $f(x)$ and impulse response $C(x_2 - x_1)$ such that the output is $f(x)$ with a change in gain given by λ. It is well-known that this requirement can be met by making $f(x) = \mathrm{e}^{\mathrm{i}\omega x}$. Substituting this into Equation (19) yields

$$\lambda = \int_{-\infty}^{\infty} C(x_2 - x_1) \mathrm{e}^{-\mathrm{i}\omega(x_2 - x_1)}\, \mathrm{d}x_1 = S(\omega) \tag{20}$$

Thus the eigenvalue is given by the power spectral density $S(\omega)$ in which ω is frequency in radians. For the case of a finite long process defined in $[-a, a]$ where a is large, it can be shown that [8]

$$\lambda_k \approx S(\omega_k) = S\left(\frac{\pi k}{a}\right) \tag{21}$$

$$f_k(x) \approx \frac{1}{\sqrt{2a}} \mathrm{e}^{\mathrm{i}(\pi k/a)x} \tag{22}$$

Substituting Equations (21) and (22) into Equations (7) and (8) gives Equations (23) and (24), respectively,

$$\varpi(x, \theta) = \bar{\varpi}(x) + \sum_{k=1}^{M} \sqrt{\frac{1}{2a} S\left(\frac{\pi k}{a}\right)} \mathrm{e}^{\mathrm{i}(\pi k/a)x} \xi_k(\theta) \tag{23}$$

$$\hat{C}(x_1, x_2) = \sum_{k=1}^{M} \frac{1}{a} S\left(\frac{\pi k}{a}\right) \cos\left(\frac{\pi k(x_1 - x_2)}{a}\right) \tag{24}$$

which is the commonly used spectral representation for the simulation of a stationary Gaussian random process [e.g., 1, 2]. Thus for large a, the K–L expansion reduces to the spectral representation. This will be demonstrated numerically in Section 3.4.

3. NUMERICAL STUDY

Numerical simulation of random processes based on the K–L expansion is performed in this section to study its convergence characteristics and suitability for practical use. The exponential covariance model corresponding to first-order Markov process [Equation (11)] is selected to illustrate the effect of the length of the process, correlation parameter and the number of K–L terms on the rate of convergence. The choice of the covariance function is a practical consideration and five common models corresponding to (a) first-order Markov, (b) binary noise, (c) band-limited white noise processes (d) second-order Markov, and (e) processes with squared exponential covariance model are investigated. In addition, simulations based on the analytical and numerical solution of the Fredholm integral equation are compared. By comparing with the spectral representation method [Equations (23) and (24)], the application range of K–L expansion and its relationship with the spectral method is studied. The advantage of the K–L expansion method over the spectral method is illustrated by its efficiency in the simulation of highly correlated processes and its ease of extension to the simulation of general non-stationary Gaussian processes.

3.1. Effect of length of process, correlation parameter and number of K–L terms

Consider a zero-mean first-order Markov process defined in $[-a,a]$ with covariance function $C(x_1,x_2)=\mathrm{e}^{-|x_1-x_2|/b}$ where b is the correlation parameter (note: $\sigma^2=1$). The process is generated based on the analytical solution of the integral equation [Equation (3)] with M K–L terms kept in the expansion. The results for $a/b=1,\ 2,\ 5$ and 10, with $M=5$ are plotted in Figure 1, in which the horizontal scale represents the lag normalized by a.

It can be seen that for all the cases, the results of covariance function based on Equation (8) (denoted as theoretical) and covariance values computed based on an ensemble of 1000 sample functions of the process simulated using Equation (7) (denoted as simulated) agree well. Hence, Equation (8) will be used in all subsequent comparative studies of the covariance function.

The simulation results agree better with the target covariance function for low a/b ratio. Physically, lower a/b implies a highly correlated process and hence, a smaller number of random variables are needed to represent the random process and correspondingly, smaller number of terms in the K–L expansion. In view of the discontinuous first derivative of $C(x_2-x_1)$ at zero lag, the simulation results at that point will not be good in that vicinity. Figure 2 shows the convergence of the covariance for $a/b=1$, where the approximate covariance function using K–L expansion approaches the target covariance function as M increases. It can be seen from Figure 3 that the convergence of the variance is fast for up to 3 terms.

By comparing Equations (2) and (8), it can be seen that the difference between the target and the simulated covariance functions is due to truncation of terms, which is a function of λ_i and $f_i(x)$, for $i>M$. For a given b, it can be proved that λ_i increases with a as follows. Multiplying both sides of Equation (3) by $f_i(x_2:a)$ and integrating with respect to x_2 over the interval $[-a,a]$, where the dependence on a is now explicitly shown,

$$\lambda_i(a)=\int_{-a}^{a}\int_{-a}^{a} f_i(x_2:a)C(x_1,x_2)f_i(x_1:a)\,\mathrm{d}x_1\,\mathrm{d}x_2 \tag{25}$$

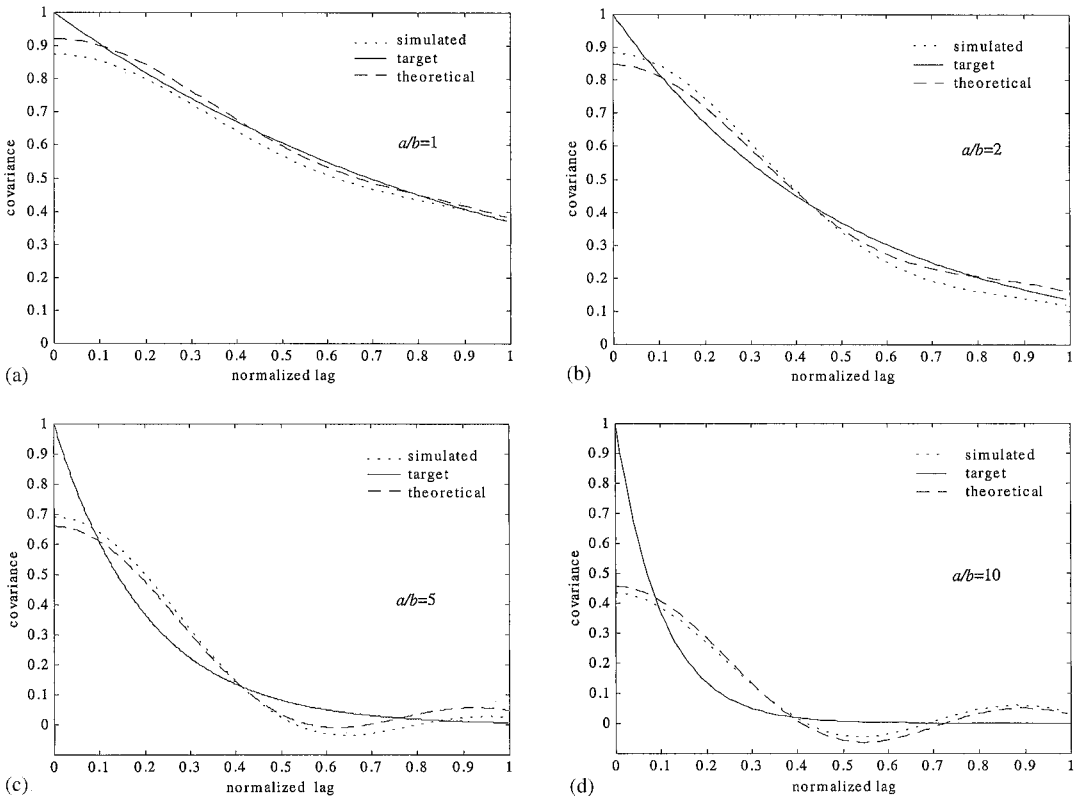

Figure 1. Comparison of simulated, target and theoretical covariance functions using $M = 5$ for: (a) $a/b = 1$; (b) $a/b = 2$; (c) $a/b = 5$; and (d) $a/b = 10$.

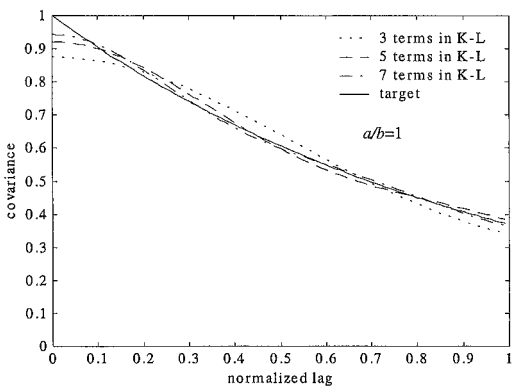

Figure 2. Convergence in exponential covariance function.

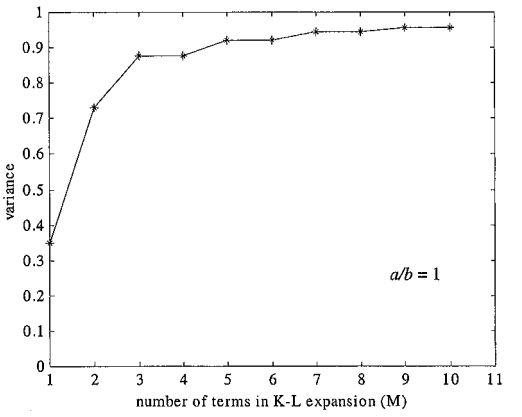

Figure 3. Convergence in variance for exponential covariance model.

Table I. Variance of K–L expansion truncated at $M = 5$ for various L/θ.

	Covariance model	
L/θ	Exponential	Sine
1	0.921	0.999
2	0.847	0.997
5	0.660	0.923
10	0.457	0.520

Note: target variance = 1.

Differentiating with respect to a and applying Equation (3),

$$\frac{\partial \lambda_i(a)}{\partial a} = 2\lambda_i(a)\left[f_i^2(a:a) + f_i^2(-a:a)\right] \geqslant 0 \tag{26}$$

This implies that $\lambda_i(a)$ is a monotone-increasing function of the length of the interval. Hence, to maintain a fixed difference between Equations (2) and (8), M has to be increased when a increases at constant b. In other words, for a given M, the accuracy decreases as a/b increases, which fully agrees with the results shown in Figure 1.

This effect is manifested more clearly when the variance is considered. To illustrate the effect of the ratio of the length of the process and the correlation parameter in a more general way, two different covariance functions are studied:

(1) Exponential covariance function $e^{-|x_1-x_2|/b}$ with $\theta = 2b$;
(2) Sine covariance function $\sin b(x_1 - x_2)/[b(x_1 - x_2)]$ with $\theta = \pi/b$.

The parameter θ, typically referred to as the scale of fluctuation, is introduced so that the correlation parameters (e.g., b) in different covariance models can be compared consistently [9]. Table I presents the variance of K–L expansion truncated at $M = 5$ for various L/θ, where L is the length of the process. As expected, the error in the variance increases with increasing L/θ. This observation can also be understood by functional analysis [10], which shows that the steeper a bilinear form decays to zero as a function of one of its arguments, the more terms are needed in its spectral representation in order to reach a specified accuracy. Noting that the Fourier transform operator is a spectral representation, it may be concluded that the faster the autocorrelation function tends to zero (that is, the smaller the scale of fluctuation θ), the broader is the corresponding power spectral density. Hence, a greater number of terms are required to represent the underlying process by K–L expansion [6].

3.2. *Effect of covariance model*

The models chosen for study are as follows: (a) first-order Markov process with exponential covariance function $e^{-|x_1-x_2|/b}$ with $b = 1$; (b) binary noise process with triangular covariance function $1 - d|x_1 - x_2|$ with $d = 1$; (c) band-limited white noise process with sine covariance function $\sin(x_1 - x_2)/(x_1 - x_2)$; (d) second-order Markov process with linear-exponential covariance function $(1 + d|x_1 - x_2|)e^{-|x_1-x_2|/b}$ with $d = 1$ and $b = 1$; and (e) random process

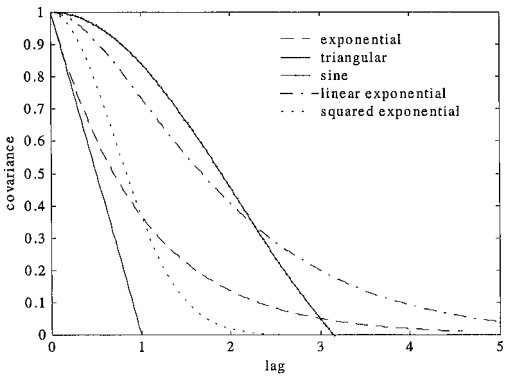

Figure 4. Commonly used covariance models.

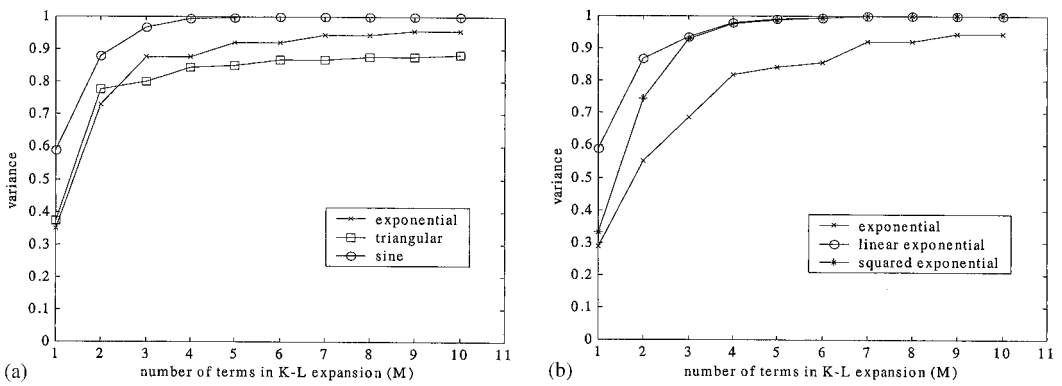

Figure 5. Convergence of variance for various covariance models using: (a) analytical solution; and (b) numerical solution of Fredholm integral equation.

with squared exponential covariance $e^{-|x_1-x_2|^2/b}$ with $b=1$. The five covariance models are illustrated in Figure 4, where for comparison purpose, L/θ is set to unity [9]. Note that the target mean and variance of all the processes are assumed to be zero and one, respectively. The covariance models (a), (b) and (c) are investigated on the basis of their analytical solution of Equation (3) whereas the covariance models (a), (d) and (e) are investigated on the basis of their numerical solution of Equation (3) [that is, using Equations (14) to (18) with polynomial basis functions].

It can be seen from Figure 5 that a smoother target covariance function (such as models (c), (d) and (e)) will have faster convergence in the variance. Note that a 'smooth' covariance function is twice differentiable at zero lag. In Figure 5(a), sine covariance (the band-limited noise process) is smooth and therefore converges faster compared to the triangular and exponential models. In Figure 5(b), the linear-exponential covariance model (second-order Markov) and the squared exponential model perform better than the exponential model for the same reason.

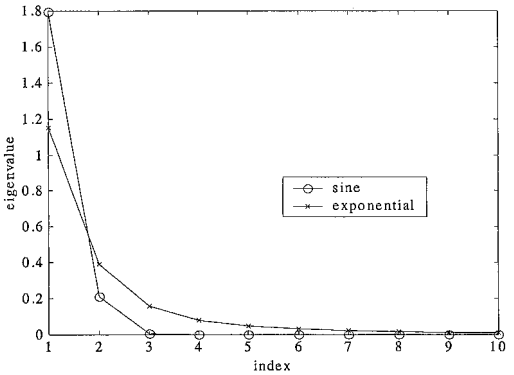

Figure 6. Decay in eigenvalues λ_i for two different covariance models ($L/\theta = 1$).

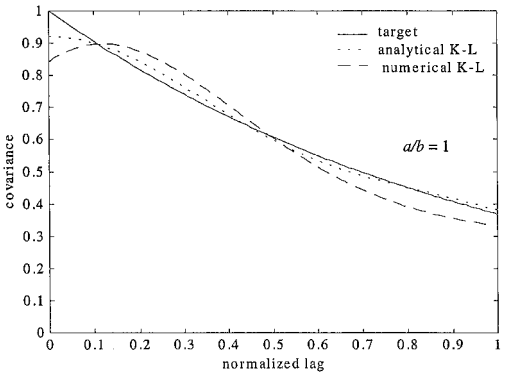

Figure 7. Comparison of analytical K–L and numerical K–L ($M = 5$) for exponential covariance model.

The above convergence behaviour can be explained in part by considering the expected energy of the process in the defined interval D, which is given by

$$E\left[\int_D [\varpi(x,\theta) - \bar{\varpi}(x)]^2 \, \mathrm{d}x\right] = \int_D C(x,x)\,\mathrm{d}x = \sum_{i=1}^{\infty} \lambda_i \tag{27}$$

Equation (27) follows from Equations (2) and (4). If the expansion is truncated after M terms, the expected energy of the simulated process is

$$E\left[\int_D [\hat{\varpi}(x,\theta) - \bar{\varpi}(x)]^2 \, \mathrm{d}x\right] = \int_D \hat{C}(x,x)\,\mathrm{d}x = \sum_{i=1}^{M} \lambda_i \tag{28}$$

The difference between Equations (27) and (28) is an indirect measure of the error in the variance. Its rate of reduction is clearly related to the rate of decay in the eigenvalues. Figure 6 compares the trend of the eigenvalues (obtained analytically) between the fully differentiable sine covariance function and the exponential covariance function that is non-differentiable at the origin. The results are consistent with those shown in Figure 5(a).

3.3. *Effect of evaluating eigen-solutions numerically*

The exponential covariance model is used to compare the difference between numerical K–L and analytical K–L. The results in Figure 2 show that for analytical K–L, $M = 5$ gives a fairly accurate solution with respect to the target covariance function and hence, Figure 7 compares the analytical K–L and numerical K–L covariance values based on $M = 5$. It can be seen that analytical K–L gives significantly better results than numerical K–L. Figure 8 shows the faster convergence of the variance for $M < 7$ using analytical K–L. Hence, by using the numerical solution to Equation (3), the effectiveness of K–L expansion is visibly reduced.

In particular, it is interesting to note from Figure 8 that the variance obtained using numerical eigen-solutions approaches the analytical version from below. One reason is that the

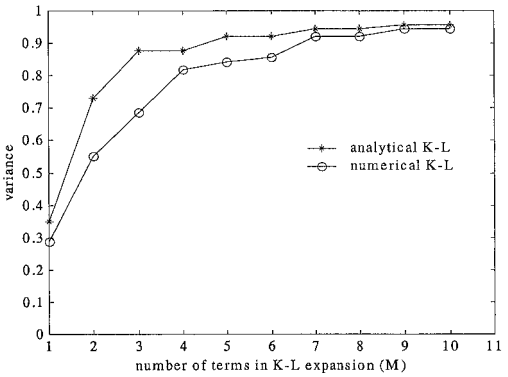

Figure 8. Comparison of variance convergence between analytical K–L and numerical K–L for exponential covariance model.

approximate eigenvalues obtained using the Galerkin method are always smaller than the actual ones [11]. This would imply that the expected energy of the process (and hence the variance) would be underestimated as discussed in Section 3.2.

3.4. Comparison with spectral representation method

The first-order Markov process is considered for simulation using both the K–L expansion [Equation (8)] and the spectral representation method [Equation (24)]. The results for $a/b = 1, 5, 10$ and 100 with $b = 1$ are shown in Figure 9. The value of M is selected so that the K–L expansion produces reasonably accurate results. As noted in Section 3.1, a larger value of M is needed for weakly correlated processes (large a/b). To ensure fair comparison, the same value of M is used for the spectral method.

Figure 10 shows the discretization of the one-sided power spectral density $G(\omega)$, which is twice $S(\omega)$ given in Equation (20). In the spectral method, the variance of the truncated process is the sum of the shaded strips associated with each discretized frequency ω_k [2]

$$\hat{\sigma}^2 = \sum_{k=1}^{M} \sigma_k^2 = \sum_{k=1}^{M} G(\omega_k)\,\Delta\omega \tag{29}$$

The variance of the actual process is the area under the entire $G(\omega)$. The error in the variance is therefore a function of the cut-off frequency, $\omega_{\max}$. For highly correlated processes (Figure 9a) K–L expansion with $M = 7$ produces very good agreement with the target covariance function, except in the vicinity of zero lag for reasons noted in Section 3.1. However, the performance of the spectral method is poor. This is because the cut-off frequency $\omega_{\max}$ is chosen to be $\pi M/a$ [Equation (21)]. When a is small, say $a = 1$ and $M = 7$, $\omega_{\max} = 7\pi$. This $\omega_{\max}$ covers only about 29 per cent of the total area under $G(\omega)$ for the exponential covariance model. The substantial power contributed by frequencies beyond $\omega_{\max}$ is not included. Hence, the result is poor when compared to K–L expansion. As a/b increases, the performance of the spectral method improves. At $a/b = 100$ (Figure 9d), the spectral method reproduces an almost exact fit to the target covariance function, even at zero lag. In this instance, $M = 1000$ and $\omega_{\max} = 10\pi$, which covers about 97 per cent of the area under $G(\omega)$.

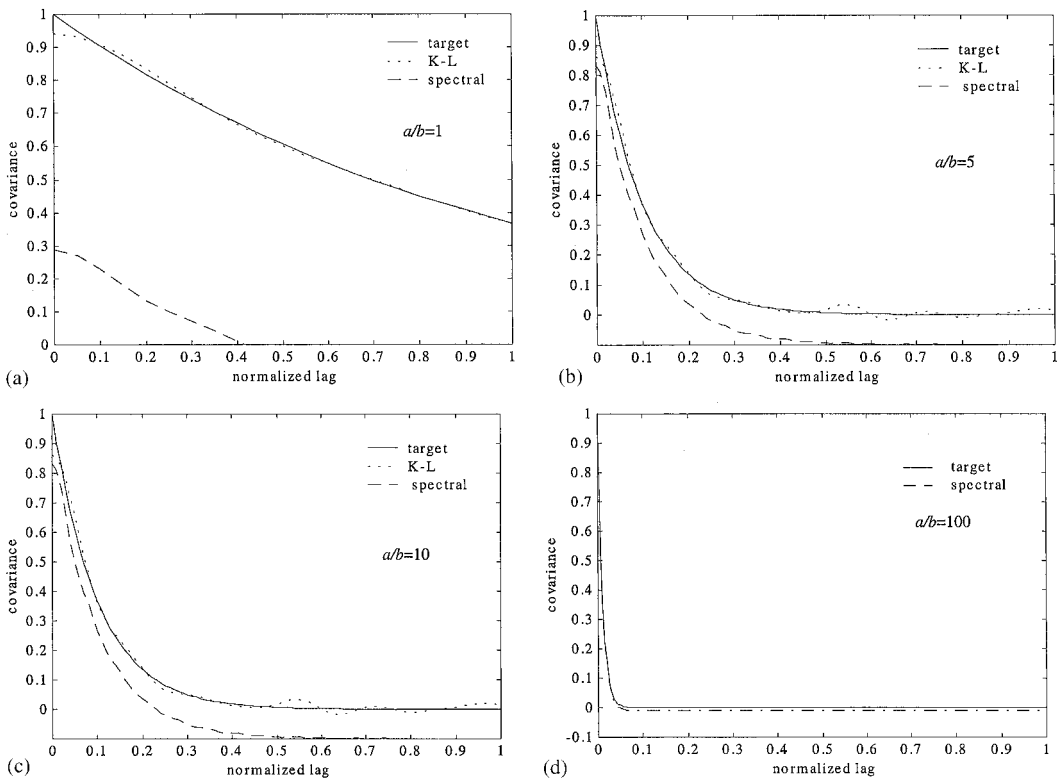

Figure 9. Comparison of covariance function of K–L expansion and spectral representation for: (a) $a/b = 1$; (b) $a/b = 5$; (c) $a/b = 10$; and (d) $a/b = 100$.

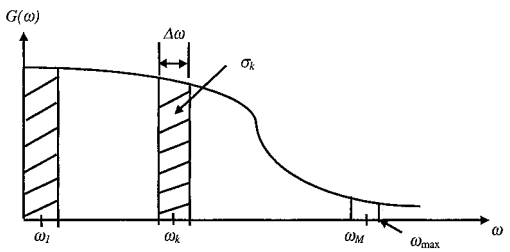

Figure 10. Discretization of power spectral density in spectral representation method.

Further, the frequencies are discretized at $\Delta\omega = \omega_{\max}/M = \pi/a$ which becomes finer when a increases. This also contributes to the improvement in the results for the spectral method as a/b increases. The corresponding K–L solution at $a/b = 100$ is not shown because very high order eigenvalues and eigenfunctions are difficult to evaluate analytically.

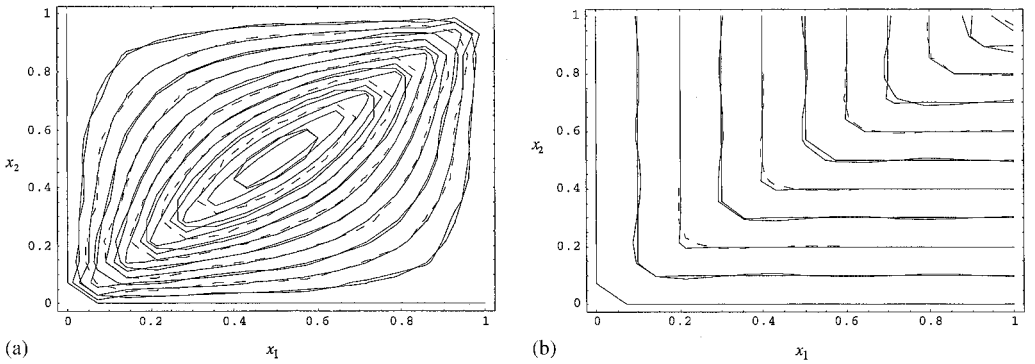

Figure 11. Comparison of target (full line) and theoretical covariance functions (dash line) using $M = 5$ for: (a) Wiener–Levy process; and (b) Brown–Bridge process.

3.5. Simulation of non-stationary process

Both the Wiener–Levy and the Brown–Bridge processes are used to illustrate the suitability of the K–L expansion method for simulating non-stationary processes. The target non-stationary processes are as follows:

(1) Wiener–Levy process in $[0, a]$ has covariance function

$$C(x_1, x_2) = \min(x_1, x_2) \tag{32}$$

(2) Brown–Bridge process defined in $[0, a]$ has covariance function

$$C(x_1, x_2) = \min(x_1, x_2) - x_1 x_2 / a \tag{33}$$

A comparison between the target covariance function and the theoretical covariance function [Equation (8)] truncated at $M = 5$ is made. The results shown in Figure 11 (contour plots) indicate good agreement and hence $M = 5$ is used for subsequent simulation. Simulation results based on 1000 samples are shown in Figure 12 which are plots for the variance. It can be seen that the simulation results agree fairly well with the target values. K–L expansion can be used to simulate non-stationary processes with any covariance function as easily and as satisfactorily as stationary processes.

4. CONCLUSIONS

K–L expansion as a representation and simulation method is investigated. If the exact eigenvalues and eigenfunctions of the covariance function can be found, K–L expansion is the most efficient method for representing the random process, i.e. it requires the smallest number of random variables to represent the random process. It is useful for stochastic finite element analysis. However, in most of the cases, closed-form eigenfunctions and eigenvalues are not available. The difficulty in solving an integral equation analytically involved in K–L expansion limits its application.

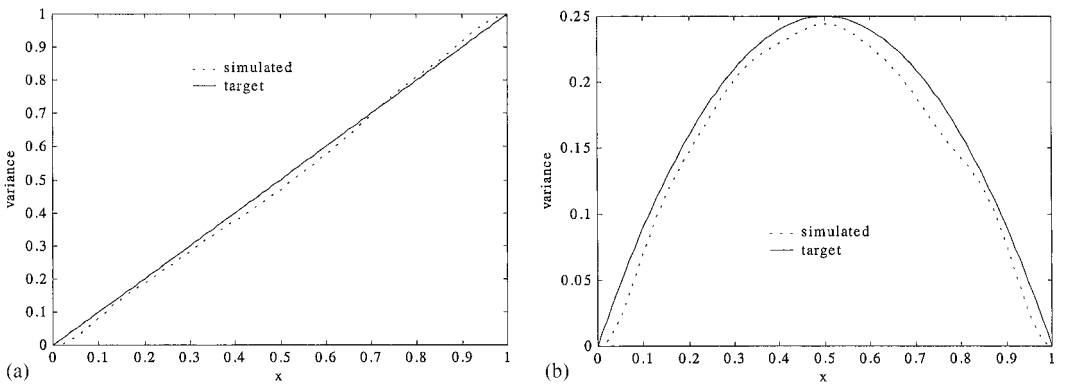

Figure 12. Comparison of target and simulated variance $C(x,x)$ using $M=5$ for: (a) Wiener–Levy process; and (b) Brown–Bridge process.

The convergence and accuracy of K–L expansion depend on the terms in the truncated K–L expansion. The lower the ratio of the length of the process over correlation parameter, the lesser are the terms needed for a given accuracy. Smooth covariance models exhibit faster convergence than models with less smooth covariance function. It is further shown that numerical K–L expansion reduces the effectiveness of the K–L expansion. In using numerical K–L expansion rather than analytical K–L expansion, more terms are needed to represent the random process for a given accuracy.

Comparison with the established and commonly used spectral representation method is made. K–L expansion has an edge over the spectral method for highly correlated processes. For long stationary processes, the spectral method is generally more efficient as the K–L expansion method requires substantial computational effort to solve the integral equation. The main advantage of the K–L expansion method is that it can be easily generalised to simulate non-stationary processes with little additional effort.

REFERENCES

1. Shinozuka M, Deodatis G. Simulation of the stochastic process by spectral representation. *Applied Mechanics Reviews*, ASME 1991; **44**(4):29–53.
2. Grigoriu M. On the spectral representation method in simulation. *Probabilistic Engineering Mechanics* 1993; **8**(2):75–90.
3. Stark H, Woods WJ. *Probability, Random Process, and Estimation Theory for Engineers.* Prentice-Hall: Englewood Cliffs, NJ, 1994.
4. Zhang J, Ellingwood B. Orthogonal series expansions of random processes in reliability analysis. *Journal of Engineering Mechanics* ASCE 1994; **120**(12):2660–2677.
5. Li CC, Der-Kiureghian A. Optimal discretization of random processes. *Journal of Engineering Mechanics* ASCE 1993; 119(6):1136–1154.
6. Ghanem R, Spanos PD. *Stochastic Finite Element: A Spectral Approach*. Springer, New York, 1991.
7. Gutierrez R, Ruiz JC, Valderrama MJ. On the numerical expansion of a second order stochastic process. *Applied Stochastic Models And Data Analysis* 1992; **8**:67–77.
8. Van Trees HL. *Detection, Estimation and Modulation Theory*, Part 1. Wiley: New York, 1968.
9. Vanmarke E.H. *Random Fields: Analysis and Synthesis*. The MIT Press, Cambridge, MA, 1984.
10. Oden JT. *Applied Functional Analysis*. Prentice-Hall: Englewood Cliffs, NJ, 1979.
11. Baker CTH. *The Numerical Treatment of Integral Equations*. Oxford University Press: Oxford, 1977.

